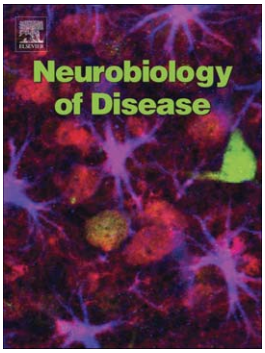

Hypothermia mediates age-dependent increase of tau phosphorylation in db/db mice

Noura B. El Khoury, Maud Gratuze, Franck Petry, Marie-Amélie Papon, Carl Julien, François Marcouiller, Françoise Morin, Samantha B. Nicholls, Frédéric Calon, Sébastien S. Hébert, André Marette, Emmanuel Planel

PII: S0969-9961(16)30005-5
DOI: doi: 10.1016/j.nbd.2016.01.005
Reference: YNBDI 3673

To appear in: *Neurobiology of Disease*

Received date: 13 October 2015
Revised date: 26 December 2015
Accepted date: 7 January 2016

Please cite this article as: El Khoury, Noura B., Gratuze, Maud, Petry, Franck, Papon, Marie-Amélie, Julien, Carl, Marcouiller, François, Morin, Françoise, Nicholls, Samantha B., Calon, Frédéric, Hébert, Sébastien S., Marette, André, Planel, Emmanuel, Hypothermia mediates age-dependent increase of tau phosphorylation in db/db mice, *Neurobiology of Disease* (2016), doi: 10.1016/j.nbd.2016.01.005

Hypothermia mediates age-dependent increase of tau phosphorylation in db/db mice

Noura B. El Khoury[a,b,1], Maud Gratuze[a,b,1], Franck Petry[a,b], Marie-Amélie Papon[b], Carl Julien[b], François Marcouiller[a,b], Françoise Morin[b], Samantha B. Nicholls[c], Frédéric Calon[b,d], Sébastien S. Hébert[a,b], André Marette[e], Emmanuel Planel[a,b,*]

[a] Université Laval, Faculté de Médecine, Département de Psychiatrie et Neurosciences, Québec, QC, Canada;

[b] Centre de recherche du Centre Hospitalier de l'Université Laval de Québec, Axe Neurosciences, Québec, QC, Canada;

[c] MassGeneral Institute for Neurodegenerative Disease, Department of Neurology, Alzheimer's Disease Research Laboratory, Massachusetts General Hospital, Harvard Medical School, Charlestown, Massachusetts, USA

[d] Université Laval, Faculté de Pharmacie, Québec, Canada

[e] Centre de Recherche de l'Institut Universitaire de Cardiologie et de Pneumologie de Québec, Quebec City, QC, Canada

[1] These authors contributed equally to this work

* Correspondence to: E. Planel, CRCHU de Québec, CHUL, P-9800, 2705 Boulevard Laurier, Québec, G1V 4G2, Canada. E-mail: emmanuel@planel.org

HIGHLIGHTS

- Type 2 diabetes enhances the risk of Alzheimer's disease.
- Tau hyperphosphorylation is a hallmark of Alzheimer's disease.
- The db/db mouse model of Type 2 diabetes has age-related tau hyperphosphorylation.
- In older mice, hypothermia is the main cause of tau hyperphosphorylation.
- Patients temperature should be included in studies between the two diseases.

ABSTRACT

Accumulating evidence from epidemiological studies suggest that type 2 diabetes is linked to an increased risk of Alzheimer's disease (AD). However, the consequences of type 2 diabetes on AD pathologies, such as tau hyperphosphorylation, are not well understood. Here, we evaluated the impact of type 2 diabetes on tau phosphorylation in db/db diabetic mice aged 4 and 26 weeks. We found increased tau phosphorylation at the CP13 epitope correlating with a deregulation of c-Jun N-terminal kinase (JNK) and Protein Phosphatase 2A (PP2A) in 4-week-old db/db mice. 26-week-old db/db mice displayed tau hyperphosphorylation at multiple epitopes (CP13, AT8, PHF-1), but no obvious change in kinases or phosphatases, no cleavage of tau, and no deregulation of central insulin signalling pathways. In contrast to younger animals, 26-week-old db/db mice were hypothermic and restoration of normothermia rescued phosphorylation at most epitopes. Our results suggest that, at early stages of type 2 diabetes, changes in tau phosphorylation may be due to deregulation of JNK and PP2A, while at later stages hyperphosphorylation is mostly a consequence of hypothermia. These results provide a novel link between diabetes and tau pathology, and underlie the importance of recording body temperature to better understand the relationship between diabetes and AD.

Keywords: Alzheimer’s disease; diabetes mellitus; db/db mice; tau hyperphosphorylation, hippocampus; kinase; phosphatase; hypothermia; temperature; thermoregulation

INTRODUCTION

Alzheimer's disease (AD) is the most prevalent neurodegenerative disorder in the elderly, accounting for 60 to 70% of all dementia cases (i.e., 47.5 million people worldwide according to the WHO 2015 report), and is thus considered one of the major public health concerns (Querfurth and LaFerla, 2010). Neuropathologically, AD is characterized by a dramatic loss of neurons in many regions of the brain, the extracellular accumulation of senile plaques composed of the amyloid-β peptide (Aβ) (Glenner and Wong, 1984), and the presence of intraneuronal neurofibrillary tangles (NFTs) consisting of abnormally hyperphosphorylated tau protein assembled in paired helical filaments (PHFs) (Grundke-Iqbal et al., 1986). Tau is a microtubule-associated protein that is abundant in the central nervous system and expressed mainly in axons. Tau hyperphosphorylation has been shown to induce PHFs and tangle formation *in vitro* (Alonso et al., 2001) and is thought to be a critical event in the pathogenesis of AD since it correlates with the degree of cognitive impairment in AD (Arriagada et al., 1992; Bretteville and Planel, 2008; Duff and Planel, 2005; Tremblay et al., 2007).

Whereas only a small proportion of AD is due to genetic mutations, the large majority of cases (~99%) is late onset and sporadic in origin. The cause of sporadic AD is not fully understood due to its multifactorial components including environmental factors that interact with biological or genetic susceptibilities to accelerate the manifestation of the disease. Interestingly, data from preclinical and clinical studies suggest that pathogenic factors involved in the development of type 2 diabetes may promote the incidence of AD (Kim et al.). Indeed, several longitudinal population-based studies have detected higher AD incidence rates in diabetic patients (Arvanitakis et al., 2004; Leibson et al., 1997; Ott et al., 1999), and type 2 diabetes was shown to affect multiple cognitive functions in patients (Roriz-Filho et al., 2009). Moreover, in comparison with age-matched control, AD patients show abnormalities in insulin and insulin receptor levels in the brain (Craft and Watson, 2004).

Over the last decade, there has been considerable interest on the impact of insulin dysfunction and diabetes on tau pathology. Studies have demonstrated that insulin is a neurotrophic factor capable of modulating tau phosphorylation both *in vitro* and *in vivo* (see (El Khoury et al., 2014) for review). Moreover, we (Papon et al., 2013; Planel et al., 2007b) and others (Clodfelder-Miller et al., 2006; Jolivalt et al., 2008; Ke et al., 2009) have reported tau hyperphosphorylation in mouse models of type 1 diabetes. Tau hyperphosphorylation has also been reported in rat (Jung et al., 2013; Li et al., 2007) and mouse (Kim et al., 2009) models of spontaneous type 2 diabetes. In addition, Liu et al. have reported higher tau hyperphosphorylation in the brains of type 2 diabetes patients (Liu et al., 2009). However, the mechanisms underlying increased tau phosphorylation in these latter models remain unclear.

Here, we investigated tau phosphorylation and its molecular mechanisms in a spontaneous model of type 2 diabetes: the db/db mouse. This is a well-established murine model bearing a mutation in the leptin receptor, which regulates adipose tissue mass through hypothalamic effects on satiety and energy expenditure (Hummel et al., 1966). Consequently, db/db mice are hyperphagic and develop obesity associated with hyperinsulinemia and severe insulin resistance (Hummel et al., 1966). Our results showed a sustained hyperphosphorylation of tau in db/db mice as early as at 4 weeks and up to 26 weeks of age. This was associated with changes in JNK and PP2A levels in 4-week-old mice but not in 26 week-old diabetic animals. Importantly, we made the novel observation that hypothermia is a consequence of type 2 diabetes in this model and that it plays a major cause in tau hyperphosphorylation since it could be reversed following normothermia.

MATERIALS AND METHODS

Animals. Male db/db (homozygous BKS.Cg-*Dock7*^{m} +/+ *Lepr*^{db}/J, stock no. 000642) were purchased from Jackson Laboratory (Bar Harbor, ME, USA) along with male heterozygotes from the colony used as control (db+). Mice were maintained in a temperature-controlled room (~23˚C) with a light/dark cycle of 12/12h, and experiments were performed during the light period. All animals had access to food and water *ad libitum*. Animals were handled according to procedures approved by the Comité de Protection des Animaux du CHU under the guidelines of the Canadian Council on Animal Care.

Monitoring of physiological parameters and metabolic features. All mice were monitored for diabetes features, notably glycemia and insulinemia. Non-fasting blood glucose was measured using a glucometer with reagent strips (ACCU-CHEK ® Aviva Nano; Roche Diagnostics GmbH, Mannheim, Germany), or a Glucose Assay Kit (Biovision Inc., Mountain View, CA, USA). Plasma insulin was determined using a sandwich enzyme immunoassay according to the manufacturer instructions (Mouse Insulin ELISA, Mercodia, Sweden). The Glucose Tolerance Test (GTT) was performed by fasting the mice for 6h (0'), and then injecting them intraperitoneally with 10% dextrose (0.1 ml/10g). For Insulin Tolerance Test (ITT), fasted mice were injected intraperitoneally with 1 U/day of insulin (Humulin R; Elli Lilly & Co., Indianapolis, IN, USA). Blood samples were collected and glucose levels were measured at different time points (0, 15, 30, 60 and 90 min) as mentioned above. All mice were weighted at sacrifice and the body temperature was monitored using a rectal probe (Thermalert TH-5, Physitemp, Clifton, NJ, USA).

Protein extraction. Mice were killed by decapitation without anesthesia, since anesthesia can increase hypothermia-induced tau phosphorylation (Planel et al., 2007a). Brains were immediately removed and tissues were dissected on ice. Hippocampal tissues were quickly weighed, frozen on

dry ice and maintained at -80˚C until they were homogenized without thawing in 5 times volume/weight of Radioimmunoprecipitation Assay (RIPA) (50 mM Tris-HCl, pH 7.4, 1% NP-40, 150 mM NaCl, 0.25% Na-deoxycholate, 1 mM EDTA, 1 mM Na_3VO_4, 1 mM NaF, 1 mM PMSF, 10 µl/ml of Proteases Inhibitors Cocktail (P8340, Sigma-Aldrich, St. Louis, MO)), using a mechanical homogenizer (TH, Omni International, Marietta, GA). Samples were then centrifuged for 20 min at 20,000 g at 4˚C. The supernatant was recovered, diluted in sample buffer (NuPAGE LDS; Invitrogen, Carlsbad, CA) containing 5% of 2-β-mercapto-ethanol, 1 mM Na_3VO_4, 1 mM NaF, 1 mM PMSF, 10 µl/ml of Proteases Inhibitors Cocktail (P8340; Sigma-Aldrich), and heated for 10 min at 95°C. Depending on the antibody used, 7–21 µg of protein were analyzed as described previously (Planel et al., 2001).

Production of TauC3. TauC3 was expressed as described in Barghorn *et al.* (Barghorn et al., 2005). A point mutation introducing a stop codon to the pET29b full-length (441 amino acids; 2N4R) Tau plasmid (addgene plasmid # 16316) at residue 422 allowed for expression of recombinant TauC3. Briefly, protein was expressed in *e.coli* strain Bl21(DE3) to an O.D. of 0.6 and induced with 1uM IPTG for four hours at 37C. The pellet was resuspended in a buffer of 20mM MES, 1 mM EGTA, 0.2 mM $MgCl_2$, 5 mM DTT, protease inhibitor cocktail (Roche), phosphatase inhibitor cocktail (sigma), pH 6.8. Cells were disrupted using sonication and boiled for 20 min at a NaCl concentration of 500 mM. The cells were then centrifuged at 127,000g for 45 min at 4C and the supernatant was dialyzed overnight into a buffer of 10 mM HEPES pH 7, 50mM NaCl. The dialysate was cleared by centrifugation at 127,000g for 45 min at 4C and loaded onto a cation exchange column. The TauC3 was eluted using a linear gradient over 6 column volumes to a final concentration of 60% 10 mM HEPES, 1M NaCl.

Western blot analysis. SDS-PAGE and Western blot analysis was done as previously described (Planel et al., 2001). All antibodies used in this study are listed in Table 1. Brain homogenates

were separated on a SDS-10% polyacrylamide gel and then transferred onto nitrocellulose membranes (Amersham Biosciences, Pittsburgh, PA). For APP analysis, proteins were separated by NuPAGE® Novex 4-12% Bis-Tris Gel (Invitrogen, Camarillo, CA, USA). Non-specific binding sites were blocked with 5% nonfat dry milk in Tris-buffered saline containing 0.1% Tween 20 for 1 hour at room temperature and then were incubated overnight at 4°C with antibodies directed against the specific antibody. The following day, membranes were washed 3 times and then incubated for 1 hour at room temperature with the corresponding secondary antibody (Petry et al., 2014) in 5% non-fat dry milk in PBS-T, and the immunoreactive signal intensity was visualized by enhanced chemiluminescence (ECL Plus, GE Healthcare Biosciences, Piscataway, NJ). Immunoreactive bands were visualized using ImageQuant LAS 4000 imaging system (GE Healthcare Biosciences, Piscataway, NJ) and densitometric analysis was performed with Image Gauge analysis software (Fujifilm USA, Valhalla, NY).

Immunofluorescence. Tissue fixation was done according to the "cold Bouin's method" previously developed in our laboratory (Planel et al., 2004). Briefly, animals were killed by decapitation, the brain was quickly removed and immersed in ice-cold Bouin's solution (saturated picric acid, formalin, acetic acid at 15:5:1) for 24 hours and embedded in paraffin blocks. Eight to ten micrometer thick sections were processed for immunohistochemical analyses. Deparaffinized and hydrated sections were incubated in Target Retrieval Solution (Dako, Carpinteria, CA) at 70°C for 25 min for enhancement of the immunoreactivity and then incubated in 7% normal goat serum, 0.2 % triton, 1% BSA in PBS 0.1 M at RT for 1 hour. The specimens were incubated with the primary antibodies diluted in PBS 0.1M containing 0.04% triton overnight at 4°C. The following antibodies were used: AT8 (1:200) and total Tau A0024 (1:500) (Table 1). Bound antibodies were visualized with Alexa Fluor 568 conjugated anti-mouse IgG (1:500) or Alexa Fluor 488 conjugated anti-rabbit IgG (1:1000) (Molecular Probes, Eugene, OR). Slices were mounted with a Vectashield Hard Set Mounting Medium containing DAPI (Vector Laboratories,

Inc, Burlingame, CA). Immunolabeled tissues were observed under a Carl Zeiss Axio Imager M2 (Jena, Germany) microscope.

Statistical analysis. Statistical analyses were performed with GraphPad Prism software 4.0. For figures 3 to 6, statistical analyses were performed using t-tests. For figures 1 and 8, statistical analysis was performed using one-way ANOVA followed by a Bonferroni's *post hoc* test, when effects were significant ($p < 0.05$) as assessed by ANOVA. For Figure 2, statistical analysis was performed using a repeated measures two-way ANOVA. $*^{/+}$, $**^{/++}$, and $***^{/+++}$ symbols indicate significant differences versus control with $p < 0.05$, $p < 0.01$, $p < 0.001$, respectively. Unless otherwise mentioned, all data are means ± SD.

RESULTS

Physiological parameters of db/db mice. In this study, we used two groups of db/db mice: aged 4 and 26 weeks. We choose these time points because they correspond to establishment of hyperglycemia and to full-blown diabetes, respectively (Kim et al., 2009). The latter point was especially chosen to allow comparison with the results of the study of Kim *et al.* (Kim et al., 2009). We first measured key physiological parameters, including weight, glycemia, insulinemia, and body temperature. As expected, db/db mice were significantly heavier than db+ controls (Fig. 1A) and had higher blood glucose (24.76 ± 3.38 *vs* 9.92 ± 0.57 mmol/L, $p < 0.0001$) and insulin (9.02 ± 2.01 *vs* 1.5 ± 0.36 µg/L, $p < 0.001$) levels already at 4 weeks of age in comparison to age-matched db+ controls (Fig. 1C and 1D). Insulin levels decreased between 4 and 26 weeks (Fig. 1D). THE DECREASE IN PLASMA INSULIN WITH AGE IS A DOCUMENTED FEATURE OF THE DB/DB MICE, LINKED TO IMPAIRED INSULIN RELEASE AND DECREASED INSULIN CONTENT IN THE ISLETS (BERGLUND ET AL., 1978). IN KIM *ET AL.* PAPER, INSULIN DROPPED BY HALF BETWEEN 8 AND 24 WEEKS OF AGE (Kim et al., 2009). Body temperature was lower but did not reach statistical significance at 4 weeks (36.5 ± 0.53 *vs* 36.96 ± 0.27°C) (Fig.1B). Interestingly, 26-week-old db/db mice showed, in addition to hyperglycemia (39.81 ± 12.24 *vs* 8.43 ± 1.29 mmol/L, $p < 0.001$) (Fig. 1C), a significant drop in body temperature (35.2 ± 1.05 *vs* 37.35 ± 0.57°C, $p < 0.001$) (Fig. 1B).

Metabolic features of db/db mice. Since insulin resistance and glucose intolerance are two major features of type 2 diabetes, we next performed Insulin Tolerance Test (ITT) and Glucose Tolerance Test (GTT) in db/db mice. ITT clearly showed insulin resistance in db/db mice at all ages (4-week-old: $p = 0.001$; $F = 8.146$; and 26-week-old: $p < 0.001$; $F = 15.90$) in comparison to db+ controls (Fig. 2A-C). Similarly, the GTT (Fig. 2B-D) showed glucose intolerance in db/db mice (4-week-old: $p=0.0496$; F = 2.674; and 26-week-old $p=0.0469$; F = 2.831).

Increased tau phosphorylation in the brain of db/db mice. We next tested whether type 2 diabetes induced tau phosphorylation in the hippocampus, using several phospho-tau antibodies (Table 1). At 4 weeks of age, we observed a significant change at the tau CP13 (pS202) epitope only (Fig. 3A3), compared to db+ control mice. On the other hand, CP13, AT8 and PHF-1 tau phospho-epitopes were higher at 26 weeks of age (Fig. 3B1,2,6), demonstrating an exacerbation of tau hyperphosphorylation with age. No changes were detected in total tau levels at these time points (Fig. 3B8). Tau is normally an axonal protein (Binder et al., 1985), although it accumulates in the somatodendritic compartment in AD (Delacourte et al., 1990). In older mice, we confirmed tau hyperphosphorylation at the AT8 epitope by immunofluorescence, but there was no somatodendritic relocalization of tau (Fig. 4).

Tau kinases in db/db mice. We next sought to determine the molecular mechanisms underlying tau hyperphosphorylation in db/db mice. We first examined the activation profiles of major tau kinases. These include glycogen synthase kinase-3β (GSK-3β), mitogen-activated protein kinase/extracellular signal-regulated kinase (MAPK/ERK), c-Jun N-terminal kinase (JNK) and cyclin-dependent kinase 5 (cdk5) (Noble et al., 2013). In 4-week-old db/db mice, we observed an increase of JNK activation (Fig. 5A6). There was also an increase of GSK-3β phosphorylation at Ser9, which actually reflects its inhibition (Fig. 5A2). In 26-week-old db/db mice, a different picture was observed. Here, we detected lower cdk5 and AMPK expression, which could not explain tau hyperphosphorylation observed at this age (Fig. 5B7,9). Thus, we identified one kinase (JNK) susceptible to cause tau hyperphosphorylation at 4 weeks in the mutant mice.

Tau phosphatases in db/db mice. As our prior results failed to explain all the effects on tau hyperphosphorylation, we next turned to tau phosphatases (PP), including PP1, PP2A, PP2B (calcineurin), and PP5 (Liu et al., 2005). Here, we observed a small but significant increase in the expression of PP2B at 4 weeks only (Fig. 6A2), but his observation is inconsistent with a role for

this PP in tau phosphorylation regulation in the db/db model. PP2A is a heterotrimeric holoenzyme consisting of a core dimer composed of a 36 kDa catalytic subunit (C) tightly bound with the scaffolding 65 kDa subunit termed PR65 or A, and this core dimer associates with a variable regulatory B subunit. Moreover, PP2A activity is enhanced by the methylation of its catalytic subunit (PP2A-C), and is conversely decreased by its demethylation (Janssens and Goris, 2001). We thus investigated the levels of PP2A-A, PP2A-Bα, PP2A-Bβ, PP2A-C, and D PP2A-C (demethylated, inactivated) expression levels in db/db mice. We observed a small but significant increase in the expression of the A scaffolding subunit together with a decrease of the catalytic subunit (PP2A-C) expression in db/db mice at 4 weeks of age (Fig. 6A3,4). No changes were observed at 26 weeks of age (Fig. 6B). Thus, we identified a reduction of PP2A-C that could contribute to increased tau phosphorylation at 4 weeks, but not at 26 weeks.

Insulin signaling in db/db mice. In addition to the deregulation of kinases and phosphatases, impaired central insulin signaling can induce tau hyperphosphorylation (Deng et al., 2009; El Khoury et al., 2014). To address this possibility, we investigated the activation state of the insulin receptor (IR), as well as Akt and PI3K kinases, three major proteins implicated in both central and peripheral insulin signaling. Interestingly, Akt can also phosphorylate tau (Ksiezak-Reding et al., 2003). Phosphorylation levels on Tyrosine 972 of IR were slightly increased in 26-week-old db/db mice but not Akt or PI3K kinases (Fig. 7A). However, there was no obvious change in the total levels of IR as well as Akt and PI3K profiles (Fig. 7), suggesting no impairment of central insulin signaling to the PI3K/Akt pathway.

Effect of normothermia on tau phosphorylation in db/db mice. We have previously demonstrated that hypothermia leads to tau hyperphosphorylation in mice (Planel et al., 2007b). As the older mice were hypothermic, we wanted to explore the role of temperature on tau phosphorylation in type 2 diabetes. We thus placed 26-week-old db/db mice in a ventilated

incubator at 34˚C for 1 hour prior to sampling. Animals incubated at 34˚C had rectal temperature equivalent to the control group, and did not become hyperthermic (data not shown). Tau hyperphosphorylation at both AT8 and CP13 epitopes was completely reversed by restoring db/db mice to normothermia (Fig. 8A,B). Tau PHF-1 epitope was only partly rescued under these conditions, suggesting that PHF-1 has a different kinetic of dephosphorylation (Fig. 8C).

Tau cleavage by caspase 3 in db/db mice. In addition to tau phosphorylation, tau cleavage is thought to play a role in AD pathology (Gamblin et al., 2003). Furthermore, a previous study detected increased tau cleavage at Asp421 with the TauC3 antibody in db/db mice at 26 weeks of age (Kim et al., 2009). Consistent with previous observations, we first thought we found evidence for increased cleavage of tau in db/db mice at 26 weeks of age using the same antibody (Fig. 9A). However, after using appropriate controls, including tau knock-out mice (TKO), recombinant Tau cleaved by caspase 3 (Fig. 9A), and secondary antibodies only (Fig. 9B), we found no specific signals for endogenous tau (in comparison to heavy and light chains of immunoglobulins). We also found no signal around 50kD (the expected molecular weight of tau) in either db/db mice or TKO mice when using a secondary antibody that recognizes only the light chain of immunoglobulins at 25kD (Fig. 9C). As tau truncation is also an important post-translational modification in AD (Derisbourg et al., 2015; Kovacech and Novak, 2010), we also examined C and N-terminal tau fragments but could not find evidence of tau truncation in 26 week-old db/db mice (Figure S1).

DISCUSSION

Many longitudinal population-based studies have detected higher AD incidence rates in type 2 diabetes patients (Arvanitakis et al., 2004; Leibson et al., 1997; Luchsinger et al., 2005; Ott et al., 1999; Peila et al., 2002). Indeed, it is now well established that diabetes is an important risk factor in AD with 29% of co-morbidity between these two diseases according to the 2014 Alzheimer's Association report. AD and type 2 diabetes are two diseases in expansion Worldwide; it is therefore essential to better understand the links between these diseases in order to develop new therapeutic and preventive strategies.

We thus used a well-established type 2 diabetes mouse model -the db/db mice- characterized by leptin receptor deficiency, weight gain, severe hyperglycemia and insulin resistance (Hummel et al., 1966). We first investigated tau phosphorylation in db/db mice in comparison with db+ controls at 4 weeks of age, and found increased tau phosphorylation at the CP13 epitope. On the other hand, there was hyperphosphorylation at CP13, AT8 and PHF-1 epitopes at 26 weeks of age. AT8 (Ser^{202}/Thr^{205}) is an antibody routinely used for the staging of AD-associated neurofibrillary pathology (Braak et al., 2006), and the phosphorylation sites detected by CP13 (Ser^{202}) and PHF-1 (Ser^{396}/Ser^{404}) are associated with paired-helical filament and neurofibrillary tangle pathology (Kimura et al., 1996). Importantly, tau Ser^{202} and Ser^{396} were found to be hyperphosphorylated in the brains of patients with type 2 diabetes (Liu et al., 2009). Thus, our results confirm and extend previous reports (Kim et al., 2009; Li et al., 2012; Ramos-Rodriguez et al., 2014), and suggest that type 2 diabetes in db/db mice leads to a biochemical pattern of tau phosphorylation similar to that seen in AD, with hyperphosphorylation at multiple epitopes at different time points during the progression of diabetes. This increased tau phosphorylation is most likely a consequence of type 2 diabetes rather than a direct effect of lack of the leptin receptor because it has been observed other models of type 2 diabetes (El Khoury et al., 2014).

While increased tau phosphorylation has been previously reported in db/db mice (Kim et al., 2009; Li et al., 2012; Ramos-Rodriguez et al., 2014), to date, there is no systematic exploration of the underlying mechanisms. Here, we investigated the causes of tau hyperphosphorylation in terms of central insulin dysfunction, dysregulation of tau kinases and phosphatases, and compromised thermoregulation.

Beside its role in regulating glucose metabolism, there is increasing evidence supporting a role of insulin in normal brain function, including control of nutrient homeostasis, reproduction, cognition and memory, as well as the regulation of tau phosphorylation (El Khoury et al., 2014). Therefore, we first attempted to elucidate whether tau hyperphosphorylation in db/db mice might be a consequence of a dysregulation of central insulin-signaling pathways. We did not detect a downregulation in insulin signaling in the brains of 24-week-old mice (ERK/MAPK, GSK-3β, Fig. 4B; IR, Akt, PI3k, Fig. 6), despite peripheral insulin resistance. Similar results were reported in db/db mice (Jolivalt et al., 2008), but also in a model of high-fat diet-induced type 2 diabetes (Gendron et al., 2013; Leboucher et al., 2013), supporting our results that the extensive tau hyperphosphorylation observed in older db/db mice is not a consequence of central insulin dysfunction.

To further explore the mechanism(s) of the observed tau hyperphosphorylation, we analyzed the expression and activation of the major tau kinases and phosphatases. At 4-weeks of age, we noticed a deregulation of JNK and PP2A that might account for increased tau phosphorylation at the CP13 epitope. These results extend previous observation of JNK activation at 12 and 24 weeks of age made in db/db mice (Jung et al., 2013; Li et al., 2012). However, in our hands, these changes were transient since there was no deregulation of tau kinases or phosphatases tested in our mice at 26 weeks of age. Therefore, our results suggest that tau hyperphosphorylation observed in db/db mice at that later age is not due to a deregulation of kinases or phosphatases.

If there is no activation of kinase and no inhibition of phosphatase, by what mechanisms tau phosphorylation might be altered? One possibility is O-linked N-acetylglucosamine (O-GlcNAc) tau modifications. In fact, O-GlcNAcylation has been shown to regulate phosphorylation of tau by competing for serine/threonine residues, with low glucose metabolism leading to less O-GlcNAcylation and more tau phosphorylation in the mouse brain (Liu et al., 2004). In contrast, an increase in O-GlcNAc protein modifications has been observed in the central nervous system of db/db mice (Xu et al., 2014), suggesting that O-GlcNAcylation might not be involved in the hyperphosphorylation of tau in these mice.

Another possibility is hypothermia. Indeed, we have shown that lower temperatures promote tau phosphorylation by acting directly on the enzymatic activities, inhibiting tau kinases linearly, and tau phosphatases exponentially, which results in a shift in phosphorylation equilibrium towards hyperphosphorylation (Planel et al., 2004). At 26 weeks of age (but not at 4 weeks), db/db mice developed hypothermia correlating with enhanced phosphorylation at multiple epitopes. Moreover, this increased phosphorylation was mostly reversible with the return of mice to normothermia, suggesting that in older db/db mice, type 2 diabetes led to tau hyperphosphorylation through hypothermia. As none of the previous studies investing tau phosphorylation in db/db mice have reported the temperature of their mice, these results underscore the need to carefully monitor body temperature when studying tau phosphorylation and its mechanisms in metabolic disorders.

Impaired thermoregulation and consequent hypothermia is well documented in experimental diabetes (Kilgour and Williams, 1996; Shalaby et al., 1989), including db/db mice (Trayhurn, 1979). We have previously shown that hypothermia in both induced (with streptozotocin) and spontaneous (Non-obese diabetic mice) mice models of type 1 diabetes lead to tau hyperphosphorylation (Papon et al., 2013; Planel et al., 2007b), but it is the first time that it is linked to tau hyperphosphorylation in a model of type 2 diabetes. Hypothermia can be a complication of human diabetes as diabetics with neuropathy have impaired thermoregulation

(Scott et al., 1987). In diabetic patients, hypothermia has been reported as early as the 19th century with temperatures as low as 34.7˚C (Foster, 1869). In a prospective study of 134 cases of hypothermia, Neil *et al.* have reported that 17% the patients were diabetic, with 65% of them with body temperatures below 33˚C, and as low as 26˚C (Neil et al., 1986). As hypothermia induces an 80% increase in tau phosphorylation for each degree Celsius below 37˚C (Planel et al., 2004), it is possible that it contributes to tau hyperphosphorylation in even mildly hypothermic diabetic patients. Thus, our results suggest that hypothermia induced by diabetes might accelerate tau pathology and contribute to the reported risk of development of AD and dementia in type 2 diabetes patients (Arvanitakis et al., 2004; Leibson et al., 1997; Ott et al., 1999). Thus, it would be interesting for future epidemiological studies to include the temperature of the diabetic patients and investigate whether hypothermic patients have more incidence of AD or other neurological problems.

Along with tau hyperphosphorylation, another early event in AD pathogenesis is the cleavage of tau by caspases (Rissman et al., 2004). Kim *et al.* have reported an apparent increase of tau cleavage by caspase 3 in db/db mice, with 2 fragments around 50kD and 25kD (Kim et al., 2009). Therefore, we wanted to replicate their results in our 26-week-old db/db mice by using the same antibody for cleaved tau. However, our data strongly suggest that the cleaved tau signals observed in db/db mice by Kim *et al.* is due to non-specific signals attributable to higher concentrations of immunoglobulins (Ig) in the brains of db/db mice in comparison with db+ controls. Indeed, we found a similar pattern when using only anti-mouse secondary antibody without primary antibody, and also in tau knock-out samples, with bands at 50kD and 25kD. Although we do not know why there is more Ig, our results are consistent with the study of Shuai *et al.* showing higher levels of Ig deposition in the brains of db/db mice (Shuai et al., 2012). Thus, our data strongly suggest that the reported tau cleavage in db/db mice is an experimental artifact due to more Ig in the brains of older db/db mice.

In this study, we investigated the impact type 2 diabetes on tau phosphorylation *in vivo*. We used the well-established db/db mouse model, characterized by weight gain, severe hyperglycemia and insulin resistance, two major features of type 2 diabetes (Hummel et al., 1966). Overall, our results indicate that, in db/db mice, type 2 diabetes leads to early changes in tau phosphorylation probably linked to deregulation of JNK and PP2A, while later hyperphosphorylation is mostly a consequence of diabetes-induced hypothermia. These results provide a novel link between type 2 diabetes and tau pathology, and underlie the importance of recording body temperature to better understand the relationship between diabetes and AD.

CONFLICT OF INTEREST

The authors declare no competing financial interests.

ACKNOWLEDGMENTS

We thank Dr. Peter Davies (Albert Einstein University, New York, NY, USA) for the generous gift of antibodies. This work was supported by Biomedical Doctoral Awards from the Alzheimer Society of Canada (to N.E.K. and M.G.), Postdoctoral Awards from the Alzheimer Society of Canada and the Alzheimer Society of Saskatchewan (to C.J.) and grants to E.P. from the Canadian Institute of Health Research (MOP-106423, PCN-102993), Fonds de Recherche en Santé du Québec (16205, 20048) and the Natural Sciences and Engineering Research Council of Canada (354722). A.M. holds a CIHR/Pfizer research Chair on the pathogenesis of insulin resistance and cardiovascular diseases. A.M., F.C. and S.S.H. were funded by grants from the CIHR. The funders had no role in study design, data collection and analysis, decision to publish, or preparation of the manuscript.

FIGURE LEGENDS

Table 1. Antibodies used in this study.

Figure 1. Physiological parameters of db/db mice. (A) body weight, (B) rectal temperature, (C) glycemia, and (D) insulinemia. Data are mean (n=5-10 for each condition) ± SEM. Asterisks indicate significant differences from db+ controls, with *** $p < 0.001$. Crosses indicate significant differences of 26-week-old mice (db+ and db/db) with 4-week-old db + controls, with $^{++}$ $p < 0.01$ and $^{+++}$ $p < 0.001$.

Figure 2. Insulin Tolerance Test (ITT) and Glucose Tolerance Test (GTT) in db+ and db/db mice. (A-C) blood glucose levels during ITT presented as percentage from baseline at 4 (A) and 26 (C)-week-old. Significant difference between db+ and db/db were revealed by repeated measures two-way ANOVA at 4-week-old ($p = 0.001$; $F = 8.146$; Df = 4) and 26-week-old ($p < 0.001$; $F = 15.90$; Df = 4). (B-D) Blood glucose levels during GTT presented as percentage from baseline at 4 (B) or 26 (D) weeks of age. Significant difference between db+ and db/db were revealed by two-way ANOVA for repeated measures at 4-week-old (p=0.0496; F = 2.674; Df = 4) and 26-week-old (p=0.0469; F = 2.831; Df = 4). Data are means (n=5 for each condition) ± SEM.

Figure 3. Western blot analysis of tau protein and phosphorylation in db/db mice. Proteins from 4 weeks (A) or 26 weeks of age (B) were extracted from mice hippocampi, separated by SDS-PAGE, and identified with the following antibodies: 1. loading control β-tubulin, 2. AT8, 3. CP13, 4. AT180, 5. pS199, 6. PHF1, 7. pS422 and 8. Total Tau. For each condition, 2 representative data are displayed with db+ (n = 5), or db/db (n=5). Representative lanes from the same blot were removed and the remaining lanes were spliced together. Data are means ± SD. Asterisks indicate significant differences from controls, with * $p < 0.05$, ** $p < 0.01$ and *** $p < 0.001$.

Figure 4. Regional anatomical localization of phosphorylated tau protein in 26-week-old db/db mice. Unmixed fluorescent photomicrographs of hippocampal sagittal sections are shown with AT8 (Red, A, B), Total Tau (Green, C, D), or merged with DAPI (E, F), for the following conditions: control (db+ mice, A, C, E) or diabetics mice (db/db mice, B, D,F). All images were taken at original magnification x5.

Figure 5. Western blot analysis of tau-related kinases in db/db mice. Proteins from 4 weeks (A) or 26 weeks of age (B) were extracted from mice hippocampi, separated by SDS-PAGE, and identified with the following antibodies: 1. GSK-3β , 2. GSK-3β p-S9 (P-S9), 3. ERK, 4. pERK, 5. JNK, 6. p-JNK, 7. cdk5, 8. p35/p25, 9. AMPK, 10. P-AMPK, 11. PKA and 12. P-PKA. For each condition, 2 representative data are displayed with db+ (n = 5), or db/db (n=5). Representative lanes from the same blot were removed and the remaining lanes were spliced together. Data are means ± SD. Asterisks indicate significant differences from controls, with * $p < 0.05$, ** $p < 0.01$ and *** $p < 0.001$.

Figure. 6. Western blot analysis of tau-related phosphatases in db/db mice. Proteins from 4 weeks (A) or 26 weeks of age (B) were extracted from mice hippocampi, separated by SDS-PAGE, and identified with the following antibodies: 1. PP1, 2. PP2B, 3. PP2A-A, 4. PP2A-C, 5. Demethylated PP2A-C (D PP2A-C), 6. PP2A-Bα, 7. PP2A-Bβ and 8. PP5. For each condition, 2 representative data are displayed with db+ (n = 5), or db/db (n=5). Representative lanes from the same blot were removed and the remaining lanes were spliced together. Data are means ± SD. Asterisks indicate significant differences from controls, with * $p < 0.05$, ** $p < 0.01$ and *** $p < 0.001$.

Figure 7. Western blot analysis of insulin receptor, PI3K and Akt phosphorylation and expression in db/db mice. Proteins from 26 weeks of age were extracted from mice hippocampi, separated by SDS-PAGE, and identified with the following antibodies: A. p-IR, B. p-Akt, C. p-PI3K, D. IR-β, E. Akt and F. PI3K. Arrowheads indicate quantized signals. For each condition, 2 representative data are displayed with db+ (n = 5), or db/db (n=5). Representative lanes from the same blot were removed and the remaining lanes were spliced together. Data are means ± SD. Asterisks indicate significant differences from controls, with * $p < 0.05$, ** $p < 0.01$ and *** $p < 0.001$.

Figure 8. Impact on hypothermia on tau phosphorylation in db/db mice. Proteins from 26 weeks of age were extracted from mice hippocampi, separated by SDS-PAGE, and identified with the following antibodies: A. AT8, B. CP13, C. PHF1 and D. Total Tau. For each condition, 1 representative datum is displayed with db+ (lane 1, n = 3), and db/db during hypothermia (lane 2, n=5) or normothermia condition (lane 3, n=5). Representative lane from the same blot were removed and the remaining lanes were spliced together. Data are means ± SD. Asterisks indicate significant differences from controls, with * $p < 0.05$, ** $p < 0.01$ and *** $p < 0.001$.

Figure 9. Western blot analysis of tau cleavage by caspase 3 in db/db mice. Proteins from 26 weeks of age were extracted from mice hippocampi, separated by SDS-PAGE, and identified with the following antibodies: A. Tau-C3 with anti-mouse secondary antibody, B. anti-mouse secondary antibody only and C. Tau-C3 with light chain specific secondary antibody. For each condition, representative data is displayed with db+ mice (lane 2-6, n = 5), db/db mice (lane 7-11, n=5), negative control Tau knock-out mice (lane 1 and 12, n=2) and positive control recombinant Tau cleaved be caspase 3 (lane 13 n=1).

Figure S1. No truncation of tau in in db/db mice. Proteins from 26 weeks of age were extracted from mice hippocampi, separated by SDS-PAGE, and identified with the following antibodies: A. Total tau which recognize C-terminal of tau protein and B. Total tau which recognize N-terminal of tau protein. Immunoreactive bands were overexposed to detect possible truncated forms of tau. Two lanes from representative immunoblots are displayed for each condition. Dividing lines represent areas where lanes from the same blot were removed and the remaining lanes were spliced together. n = 5 for each condition.

REFERENCES

Alonso, A. C., et al., 2001. Hyperphosphorylation induces self-assembly of tau into tangles of paired helical filaments / straight filaments. Proc. Natl. Acad. Sci. U. S. A. 98**,** 6923-6928.

Arriagada, P. V., et al., 1992. Neurofibrillary tangles but not senile plaques parallel duration and severity of Alzheimer's disease. Neurology. 42**,** 631-9.

Arvanitakis, Z., et al., 2004. Diabetes mellitus and risk of Alzheimer disease and decline in cognitive function. Arch Neurol. 61**,** 661-6.

Barghorn, S., et al., 2005. Purification of recombinant tau protein and preparation of Alzheimer-paired helical filaments in vitro. Methods in molecular biology. 299**,** 35-51.

Berglund, O., et al., 1978. Development of the insulin secretory defect in genetically diabetic (db/db) mouse. Acta endocrinologica. 87**,** 543-51.

Binder, L. I., et al., 1985. The distribution of tau in the mammalian central nervous system. J Cell Biol. 101**,** 1371-8.

Braak, H., et al., 2006. Staging of Alzheimer disease-associated neurofibrillary pathology using paraffin sections and immunocytochemistry. Acta Neuropathol. 112**,** 389-404.

Bretteville, A., Planel, E., 2008. Tau aggregates: toxic, inert, or protective species? J Alzheimers Dis. 14**,** 431-6.

Clodfelder-Miller, B. J., et al., 2006. Tau is hyperphosphorylated at multiple sites in mouse brain in vivo after streptozotocin-induced insulin deficiency. Diabetes. 55**,** 3320-5.

Craft, S., Watson, G. S., 2004. Insulin and neurodegenerative disease: shared and specific mechanisms. Lancet Neurol. 3**,** 169-78.

Delacourte, A., et al., 1990. Pathological proteins Tau 64 and 69 are specifically expressed in the somatodendritic domain of the degenerating cortical neurons during Alzheimer's disease. Demonstration with a panel of antibodies against Tau proteins. Acta Neuropathol. 80**,** 111-7.

Deng, Y., et al., 2009. Dysregulation of insulin signaling, glucose transporters, O-GlcNAcylation, and phosphorylation of tau and neurofilaments in the brain: Implication for Alzheimer's disease. Am J Pathol. 175**,** 2089-98.

Derisbourg, M., et al., 2015. Role of the Tau N-terminal region in microtubule stabilization revealed by new endogenous truncated forms. Scientific reports. 5**,** 9659.

Duff, K., Planel, E., 2005. Untangling memory deficits. Nat Med. 11**,** 826-7.

El Khoury, N. B., et al., 2014. Insulin dysfunction and Tau pathology. Frontiers in cellular neuroscience. 8**,** 22.

Foster, B. W., 1869. The Temperature in Diabetes. Journal of anatomy and physiology. 3**,** 377-8.

Gamblin, T. C., et al., 2003. Caspase cleavage of tau: linking amyloid and neurofibrillary tangles in Alzheimer's disease. Proc Natl Acad Sci U S A. 100**,** 10032-7.

Gendron, T. F., et al., 2013. Does obesity-induced tau phosphorylation tip the scale toward dementia? Diabetes. 62**,** 1365-6.

Glenner, G. G., Wong, C. W., 1984. Alzheimer's disease: initial report of the purification and characterization of a novel cerebrovascular amyloid protein. Biochem Biophys Res Commun. 120**,** 885-90.

Grundke-Iqbal, I., et al., 1986. Abnormal phosphorylation of the microtubule-associated protein tau (tau) in Alzheimer cytoskeletal pathology. Proc Natl Acad Sci U S A. 83**,** 4913-7.

Hummel, K. P., et al., 1966. Diabetes, a new mutation in the mouse. Science. 153**,** 1127-8.

Janssens, V., Goris, J., 2001. Protein phosphatase 2A: a highly regulated family of serine/threonine phosphatases implicated in cell growth and signalling. Biochem J. 353**,** 417-39.

Jolivalt, C. G., et al., 2008. Defective insulin signaling pathway and increased glycogen synthase kinase-3 activity in the brain of diabetic mice: parallels with Alzheimer's disease and correction by insulin. J Neurosci Res. 86**,** 3265-74.

Jung, H. J., et al., 2013. Age-dependent increases in tau phosphorylation in the brains of type 2 diabetic rats correlate with a reduced expression of p62. Experimental neurology. 248**,** 441-50.

Ke, Y. D., et al., 2009. Experimental diabetes mellitus exacerbates tau pathology in a transgenic mouse model of Alzheimer's disease. PLoS ONE. 4**,** e7917.

Kilgour, R. D., Williams, P. A., 1996. Effects of diabetes and food deprivation on shivering activity during progressive hypothermia in the rat. Comp Biochem Physiol A Physiol. 114**,** 159-65.

Kim, B., et al., 2009. Increased tau phosphorylation and cleavage in mouse models of type 1 and type 2 diabetes. Endocrinology. 150**,** 5294-301.

Kimura, T., et al., 1996. Sequential changes of tau-site-specific phosphorylation during development of paired helical filaments. Dementia. 7**,** 177-81.

Kovacech, B., Novak, M., 2010. Tau truncation is a productive posttranslational modification of neurofibrillary degeneration in Alzheimer's disease. Current Alzheimer research. 7**,** 708-16.

Ksiezak-Reding, H., et al., 2003. Akt/PKB kinase phosphorylates separately Thr212 and Ser214 of tau protein in vitro. Biochim Biophys Acta. 1639**,** 159-68.

Leboucher, A., et al., 2013. Detrimental effects of diet-induced obesity on tau pathology are independent of insulin resistance in tau transgenic mice. Diabetes. 62**,** 1681-8.

Leibson, C. L., et al., 1997. Risk of dementia among persons with diabetes mellitus: a population-based cohort study. Am J Epidemiol. 145**,** 301-8.

Li, J., et al., 2012. Metformin attenuates Alzheimer's disease-like neuropathology in obese, leptin-resistant mice. Pharmacology, biochemistry, and behavior. 101**,** 564-74.

Li, Z. G., et al., 2007. Alzheimer-like changes in rat models of spontaneous diabetes. Diabetes. 56**,** 1817-24.

Liu, F., et al., 2005. Contributions of protein phosphatases PP1, PP2A, PP2B and PP5 to the regulation of tau phosphorylation. Eur J Neurosci. 22**,** 1942-50.

Liu, F., et al., 2004. O-GlcNAcylation regulates phosphorylation of tau: a mechanism involved in Alzheimer's disease. Proc Natl Acad Sci U S A. 101**,** 10804-9.

Liu, Y., et al., 2009. Brain glucose transporters, O-GlcNAcylation and phosphorylation of tau in diabetes and Alzheimer's disease. J Neurochem. 111**,** 242-9.

Luchsinger, J. A., et al., 2005. Aggregation of vascular risk factors and risk of incident Alzheimer disease. Neurology. 65**,** 545-51.

Neil, H. A., et al., 1986. Risk of hypothermia in elderly patients with diabetes. Br Med J (Clin Res Ed). 293**,** 416-8.

Noble, W., et al., 2013. The importance of tau phosphorylation for neurodegenerative diseases. Frontiers in neurology. 4**,** 83.

Ott, A., et al., 1999. Diabetes mellitus and the risk of dementia: The Rotterdam Study [see comments]. Neurology. 53**,** 1937-1942.

Papon, M. A., et al., 2013. Deregulation of Protein Phosphatase 2A and Hyperphosphorylation of tau Protein Following Onset of Diabetes in NOD Mice. Diabetes. 62**,** 609-617.

Peila, R., et al., 2002. Type 2 diabetes, APOE gene, and the risk for dementia and related pathologies: The Honolulu-Asia Aging Study. Diabetes. 51**,** 1256-62.

Petry, F. R., et al., 2014. Specificity of anti-tau antibodies when analyzing mice models of Alzheimer's disease: problems and solutions. PloS one. 9**,** e94251.

Planel, E., et al., 2004. Alterations in glucose metabolism induce hypothermia leading to tau hyperphosphorylation through differential inhibition of kinase and phosphatase activities: implications for Alzheimer's disease. J Neurosci. 24**,** 2401-11.

Planel, E., et al., 2007a. Anesthesia leads to tau hyperphosphorylation through inhibition of phosphatase activity by hypothermia. Journal of Neuroscience. 27**,** 3090-3097.

Planel, E., et al., 2007b. Insulin dysfunction induces in vivo tau hyperphosphorylation through distinct mechanisms. J Neurosci. 27**,** 13635-48.

Planel, E., et al., 2001. Inhibition of protein phosphatase 2A overrides Tau protein kinase I / glycogen synthase kinase 3beta and Cyclin-dependant kinase 5 inhibition and results in tau hyperphosphorylation in the hippocampus of starved mouse. J. Biol. Chem. 276**,** 34298-34306.

Querfurth, H. W., LaFerla, F. M., 2010. Alzheimer's disease. N Engl J Med. 362**,** 329-44.

Ramos-Rodriguez, J. J., et al., 2014. Central proliferation and neurogenesis is impaired in type 2 diabetes and prediabetes animal models. PloS one. 9**,** e89229.

Rissman, R. A., et al., 2004. Caspase-cleavage of tau is an early event in Alzheimer disease tangle pathology. J Clin Invest. 114**,** 121-30.

Roriz-Filho, J. S., et al., 2009. (Pre)diabetes, brain aging, and cognition. Biochim Biophys Acta.

Scott, A. R., et al., 1987. Diabetes mellitus and thermoregulation. Can J Physiol Pharmacol. 65**,** 1365-76.

Shalaby, T. H., et al., 1989. Thermoregulatory responses of diabetic rats. Comp Biochem Physiol A. 94**,** 153-7.

Shuai, H., et al., 2012. Role of stereotaxically injected IgG from db/db mice in the phosphorylation of the microtubule-associated protein tau in hippocampus. Brain research. 1486**,** 14-26.

Trayhurn, P., 1979. Thermoregulation in the diabetic-obese (db/db) mouse. The role of non-shivering thermogenesis in energy balance. Pflugers Archiv : European journal of physiology. 380**,** 227-32.

Tremblay, C., et al., 2007. Biochemical characterization of Abeta and tau pathologies in mild cognitive impairment and Alzheimer's disease. Journal of Alzheimer's disease : JAD. 12**,** 377-90.

Xu, C., et al., 2014. O-GlcNAcylation under hypoxic conditions and its effects on the blood-retinal barrier in diabetic retinopathy. International journal of molecular medicine. 33**,** 624-32.

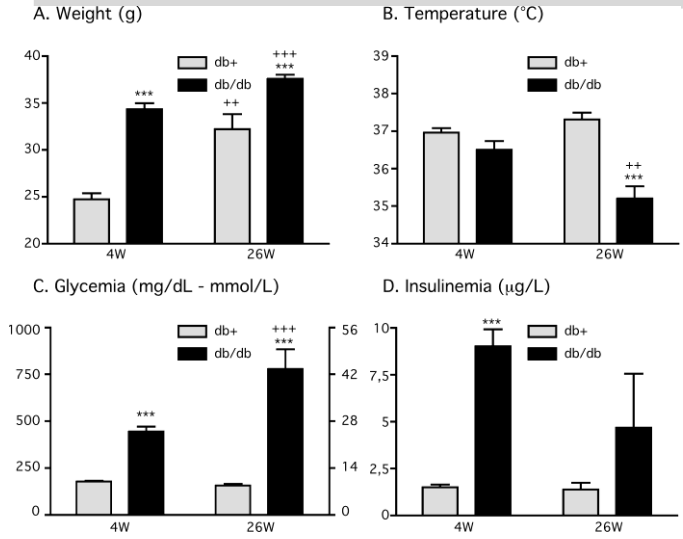

Figure 1

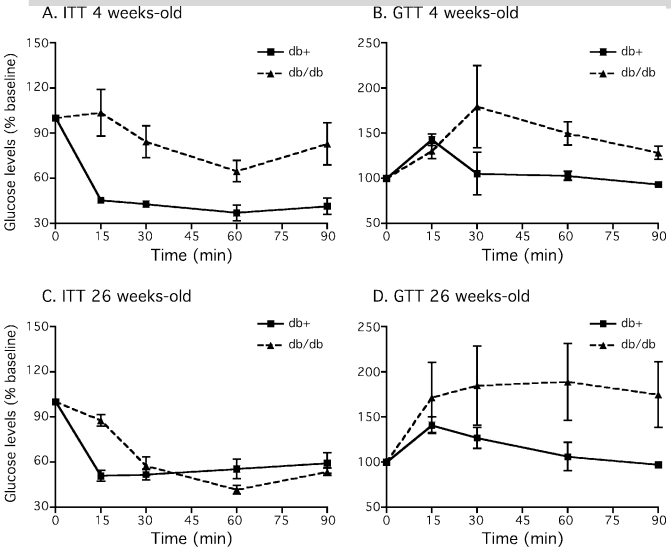

Figure 2

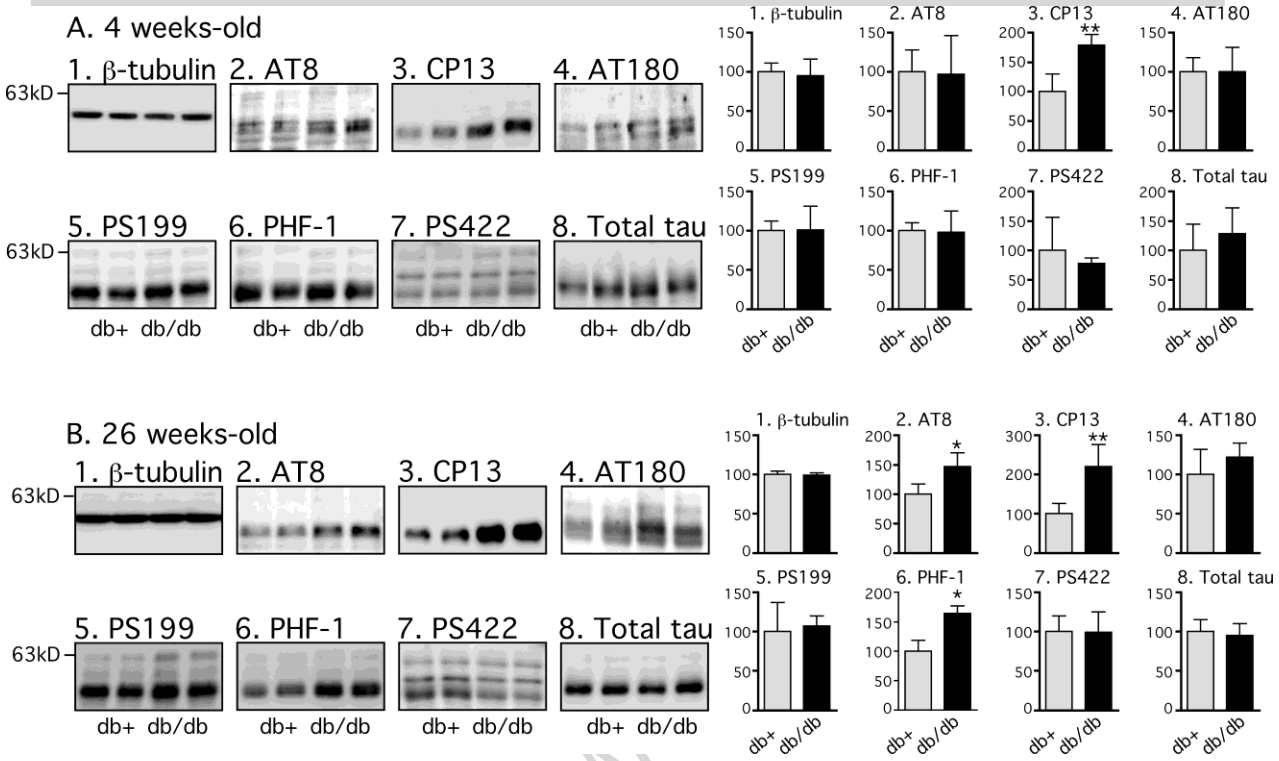

Figure 3

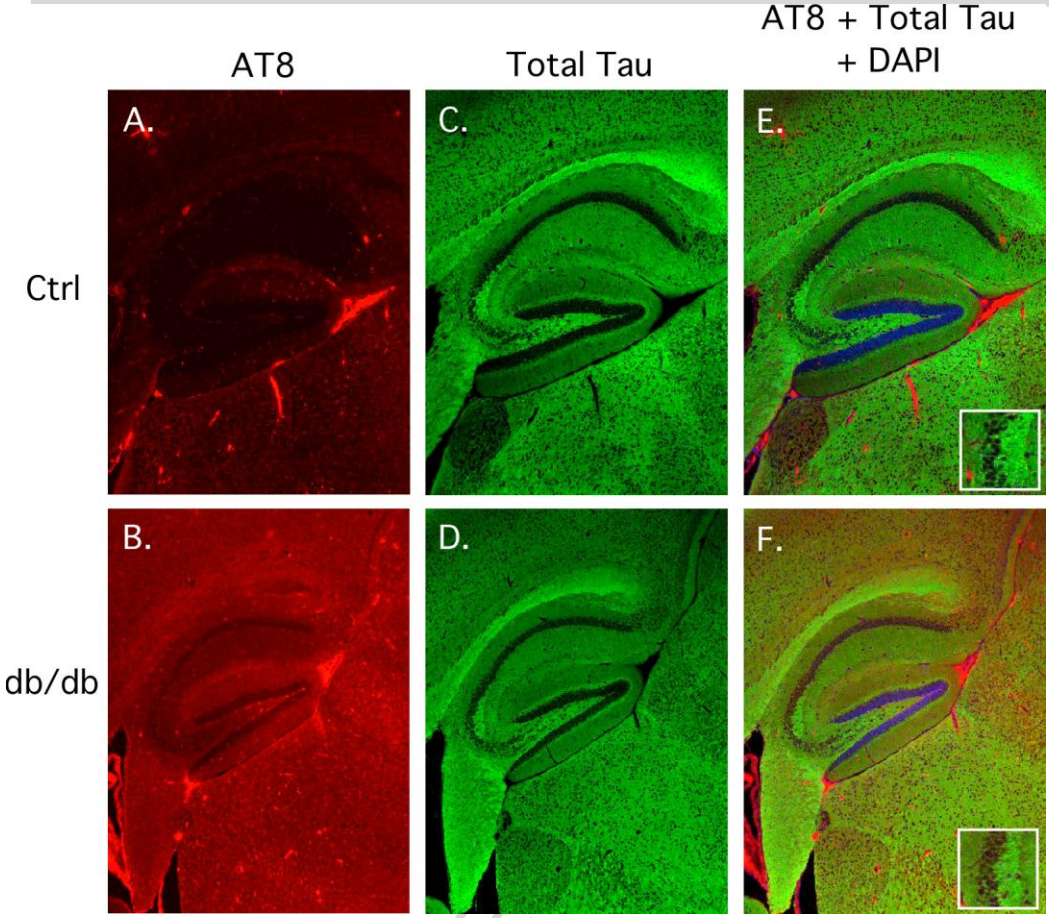

Figure 4

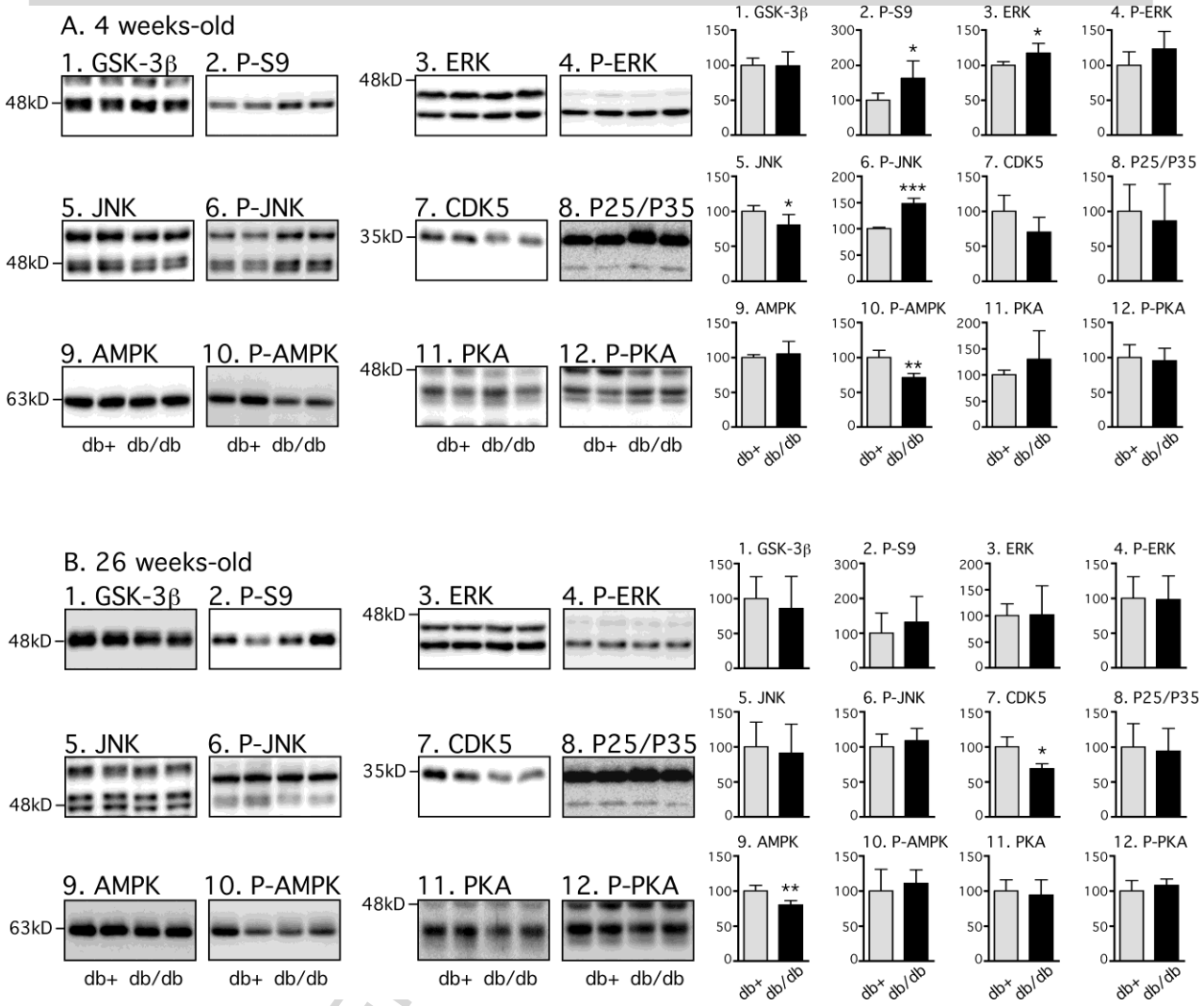

Figure 5

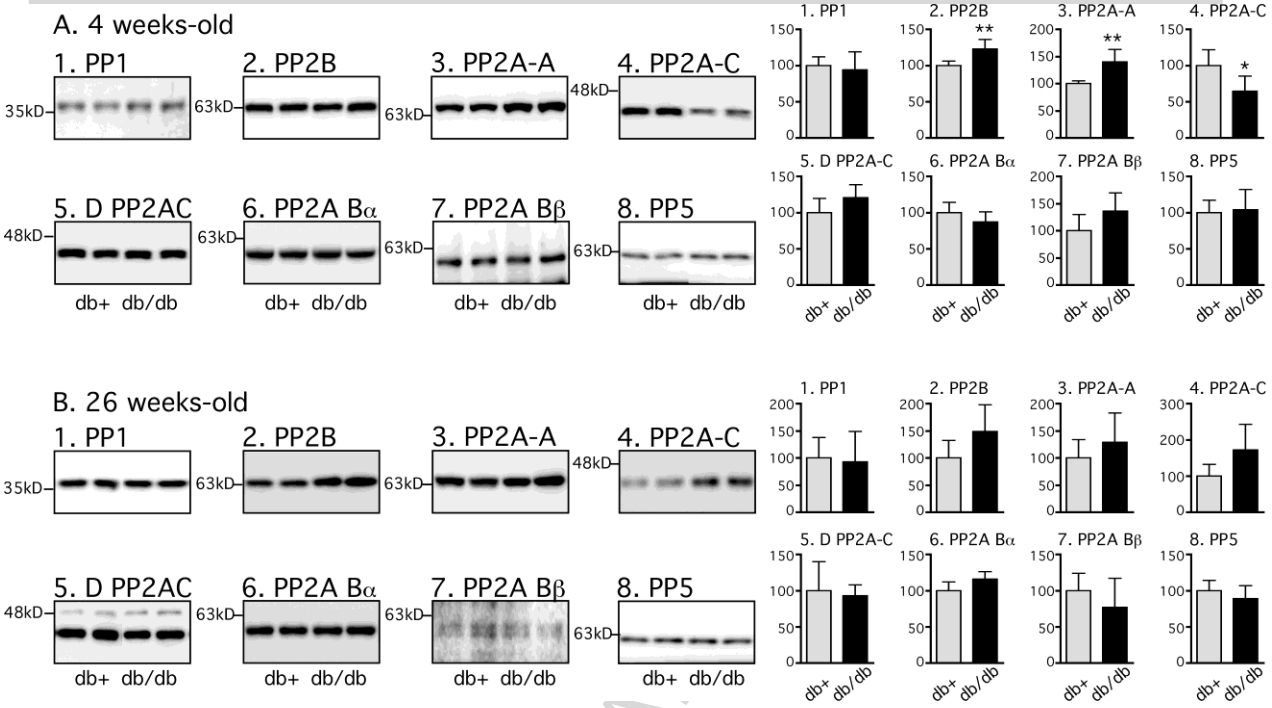

Figure 6

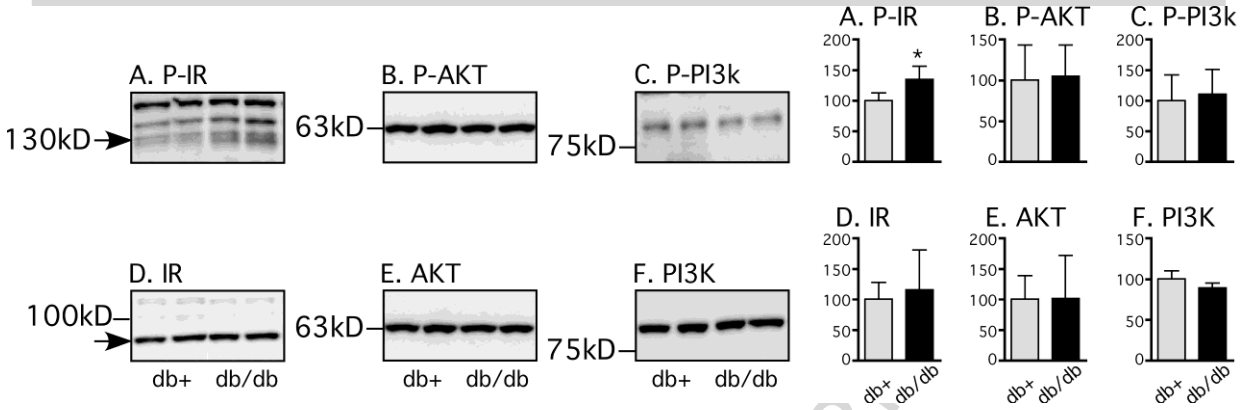

Figure 7

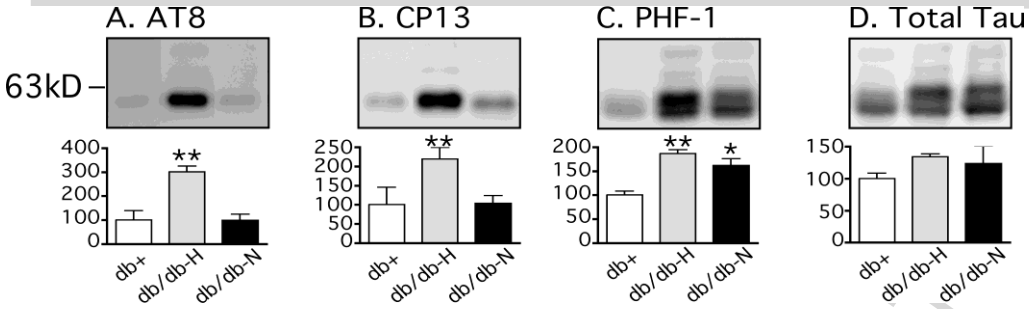

Figure 8

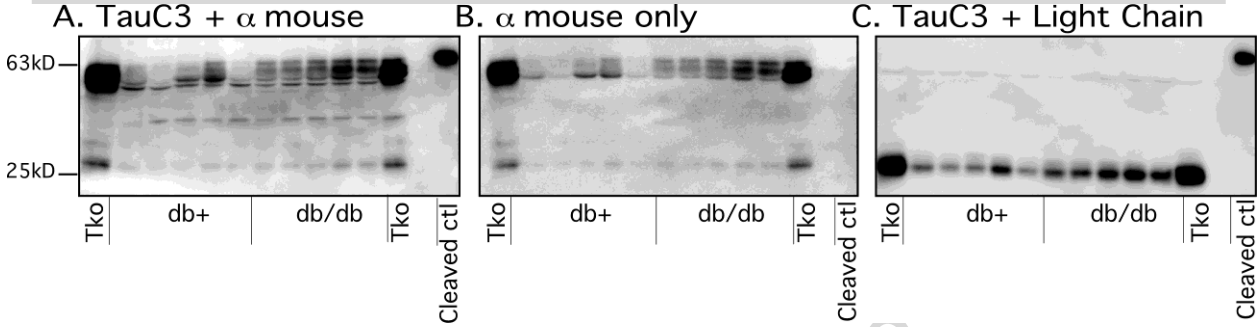

Figure 9

Table 1

Name	Abbreviation	Epitope	Type	Source	Provider	WB dilution
TAU						
Anti-Tau-1, clone PC1C6	Tau-1	pS195, pS198, pS199 and pS202	Monoclonal	Mouse	Millipore	1/1000
Anti-Phospho-PHF-tau pSer202/Thr205, Clone: AT8	AT8	pS202, pT205	Monoclonal	Mouse	Thermo Scientific	1/1000
CP13	CP13	pS202	Monoclonal	Mouse	Peter Davies	1/1000
Anti-Phospho-PHF-tau pThr231, Clone: AT180	AT180	pT231	Monoclonal	Mouse	Thermo Scientific	1/1000
Tau [pS199] Rabbit pAb	PS199	pS199	Polyclonal	Rabbit	Life Technologies	1/1000
PHF-1	PHF-1	pS396, pS404	Monoclonal	Mouse	Peter Davies	1/1000
Tau [pS422] Polyclonal Antibody, Rabbit	PS422	pS422	Polyclonal	Rabbit	Life Technologies	1/1000
DA9	Total tau N-ter	Total Tau 102-140	Monoclonal	Mouse	Peter Davies	1/10000
Anti-Human Tau A0024	Total tau	Total Tau 243-441	Polyclonal	Rabbit	Dako Cytomation	1/10000
KINASES						
GSK-3β	GSK-3βGSK-3βGSK-3β	Rat GSK-3β 1-160	Monoclonal	Mouse	BD Transduction	1/1000
Phospho GSK3β (Ser9)	GSK-3β P-S9GSK-3β P-S9GSK-3β P-S9	pS9	Polyclonal	Rabbit	Cell Signaling	1/1000
p44/p42 MAP kinase	ERK	Rat p44 MAPK C-Terminus	Polyclonal	Rabbit	Cell Signaling	1/1000
Phospho-p44/42 MAPK (Erk1/2) (Thr202/Tyr204)	P-ERK	pT202, pY204	Polyclonal	Rabbit	Cell Signaling	1/1000

SAPK/JNK	JNK	Human JNK2	Polyclonal	Rabbit	Cell Signaling	1/1000
Phospho-SAPK/JNK (Thr183/Tyr185)	P-JNK	pT183, pY185	Polyclonal	Rabbit	Cell Signaling	1/1000
Cdk5 (C-8)	CDK5	Human cdk5 C-Terminus	Polyclonal	Rabbit	Santa Cruz	1/1000
p35/25 (C64B10)	P35-25	Human p35 C-Terminus	Polyclonal	Rabbit	Cell Signaling	1/1000
AMPKa (23A3)AMPKa (23A3)	AMPK	Human AMPKa N-terminusHuman AMPKa N-terminus	Monoclonal	Rabbit	Cell Signaling	1/1000
Phospho-AMPKa (Thr172) (40H9)Phospho-AMPKa (Thr172) (40H9)	P-AMPK	pT172	Monoclonal	Rabbit	Cell Signaling	1/1000
PKAa/b/g cat (H-56): sc-98951PKAa/b/g cat (H-56): sc-98951	PKA	aa 231-286 near C-terminus of PKAaaa 231-286 near C-terminus of PKAa	Polyclonal	Rabbit	Santa Cruz	1/1000
PHOSPHATASES						
PP1 (E-9)	PP1	Human full-length PP1-α	Monoclonal	Mouse	Santa Cruz	1/1000
Pan-Calcineurin A	PP2B	Human Calcineurin A (α isofrom) C-Terminus	Polyclonal	Rabbit	Cell Signaling	1/1000
PP2A A Subunit	PP2A A	Human PP2A A subunit (α and β isoforms) C-Terminus	Polyclonal	Rabbit	Cell Signaling	1/1000
PP2A C Subunit	PP2A C	Human PP2A C subunit (α and β isoforms) C-Terminus	Polyclonal	Rabbit	Cell Signaling	1/1000
demethylated-PP2A-C (4B7)	PP2A C Dem	Unmethylated PP2A C C-Terminus	Monoclonal	Mouse	Santa Cruz	1/1000
PPP2R2A (2G9)	PP2A Bα	Rat PPP22R2A/PP2A, B55-α/PR55-α	Monoclonal	Mouse	Cell Signaling	1/1000
Anti-PP2A, B β subunitAnti-	PP2A Bβ	PP2ABβ N-TerminuesPP2ABβ	Polyclonal	Rabbit	Millipore	1/5000

PP2A, B β subunit		N-Terminues				
PP5	PP5	Human PP5 N-Terminus	Polyclonal	Rabbit	Cell Signaling	1/1000
INSULIN SIGNALING						
Anti-phospho-IR (Tyr972)	P-IR	pY972 IRa	Polyclonal	Rabbit	Millipore	1/1000
Insulin Rb (C-19): sc-711	IR	C-terminus of insulin receptor b	Polyclonal	Rabbit	Santa Cruz	1/1000
Phospho-Akt (Ser473)	P-AKT	pS473	Polyclonal	Rabbit	Cell signaling	1/1000
Akt	AKT	Mouse Akt C-Terminus (Akt1, Akt2 and Akt3)	Polyclonal	Rabbit	Cell Signaling	1/1000
Phospho-PI3K p85 (Tyr458)/p55 (Tyr 199)	P-PI3K	pY458/pY199 of PI3K (p85/p%55)	Polyclonal	Rabbit	Cell signaling	1/1000
PI3 Kinases p85 (19H8)	PI3K	Total PI3K p85 protein	Monoclonal	Rabbit	Cell Signaling	1/1000
LOADING CONTROL						
Monoclonal anti-b-tubulin clone TUB 2.1	β–τυβυλιν	β–τυβυλιν χλονε TY B 2.1	Monoclonal	Mouse	Sigma Aldrich	1/10000
SECONDARY ANTIBODIES						
Peroxidase-conjugated AffiniPure Goat Anti-Mouse IgG	Anti-Mouse	Mouse IgG	-	Goat	Jackson Immunoresearch	1/5000
Peroxidase-conjugated AffiniPure Goat Anti-Rabbit IgG	Anti-Rabbit	Rabbit IgG	-	Goat	Jackson Immunoresearch	1/5000
Mouse TrueBlot ULTRA: Anti-Mouse Ig HRP	TrueBlot	Reactive with native forms of Igs	-	Rat	Rockland	1/1000
Goat Anti-Mouse light chain Antibody, HRP conjugate	Light Chain	Reactive with native primary antibodies light chains	-	Goat	Millipore	1/5000